Theoretical Studies of Oxidative Addition of E−E Bonds (E = S, Se, Te) to Palladium(0) and Platinum(0) Complexes

Jason M. Gonzales, Djamaladdin G. Musaev,* and Keiji Morokuma*

Cherry L. Emerson Center for Scientific Computation, Department of Chemistry, Emory University, Atlanta, Georgia 30322

Received January 12, 2005

The density functional method has been applied to investigate the mechanism and controlling factors of RE−ER (R = H, Me and E = S, Se, Te) oxidative addition to $M(PR_3')_2$ complexes (where M = Pd, Pt and R′ = H, Me), which is proposed to be the first step of Pd(0)- and Pt(0)-catalyzed E−E addition to C=C and C≡C bonds. In general, it was shown that the energy of E−E activation correlates with the E−E bonding energy and decreases via the sequence E = S > Se > Te, for all R, R′ and transition-metal atoms used; the weaker the E−E bond, the smaller the oxidative addition barrier. The exothermicity of this reaction also decreases via the same trend, E = S > Se > Te, and correlates with the decrease in M−ER bond strength. Meanwhile, the E−E activation barrier is found to be higher for M = Pt than for M = Pd, while for all studied R, R′, and E the reaction is found to be more exothermic for M = Pt than for M = Pd. It was shown that the more the methyl substitution in the systems (both in substrate and the catalyst), the larger the E−E activation barrier. Calculations of the energetics of the reaction *cis*-$(PR'_3)_2Pd(ER)_2 \rightarrow$ *cis*-$(PR'_3)Pd(ER)_2 + PR'_3$ show that PR'_3 dissociation energy from the *cis*-$(PR'_3)_2Pd(ER)_2$ complex decreases (a) via the sequence E = S > Se > Te for given M and R = R′ and (b) via the trend M = Pt > Pd for given E and R = R′. The exothermicity of dimerization of the *cis*-$(PR'_3)M(ER)_2$ intermediate decreases via the sequence E = S > Se >Te and increases via M = Pd < Pt for R = R′ = H.

I. Introduction

Transition metal complex catalyzed E−X (E = heteroatom, X = H or the same or other heteroatom) addition to C=C and C≡C bonds is generally characterized by its high product yield and selectivity under mild reaction conditions and has become one of the important techniques of synthetic chemistry.[1] Previous extensive studies of B−H, B−B, B−Si,[2] B−S,[3] S−C,[4] S−Si,[5] and Se−C[3,4b,6] addition to the various alkenes and alkynes show that the mechanistic details of these reactions could be very complex and depend on the nature of E, X, transition-metal atoms and auxiliary ligands. One of the elementary reactions involved in these multistep and complex transformations is suggested to be the oxidative addition of the E−X bond to the transition-metal complex, a process that could be very complex.

Indeed, recently reported Pd(0)- and Pt(0)-catalyzed S−S and Se−Se addition to alkynes, which leads to *Z*-substituted alkenes with high stereoselectivity, occurs much faster for M = Pd than for M = Pt.[7] Furthermore, although the oxidative addition of S−S and Se−Se bonds to Pd(0) complexes leads to the dimer product $(PR'_3)(ER)Pd(\mu\text{-}ER)_2Pd(ER)(PR'_3)$, their addition to the analogous Pt(0) complexes resulted only in the monomer complexes $(ER)_2M(PR'_3)_2$. Similarly, Albano and co-workers have also reported the oxidative addition of Se−Se bonds to Pt(0) complexes, such as Pt(dmphen)(olefin), where dmphen = 2,9-dimethyl-1,10-phenanthroline, leading to *trans*-$Pt(SeR)_2$(dmphen)(olefin) species.[8] However, these extensive experimental studies left unknown several issues related to the mechanisms, as well as the

* To whom correspondence should be addressed. E-mail: dmusaev@emory.edu (D.G.M.); morokuma@emory.edu (K.M.).

(1) *Catalytic Heterofunctionalization*; Togni, A., Grützmacher, H., Eds.; Wiley-VCH: Weinheim, Germany, 2001.

(2) (a) Alonso, F.; Beletskaya, I. P.; Yus, M. *Chem. Rev.* **2004**, *104,* 3079. (b) Beletskaya, I. P.; Moberg, C. *Chem. Rev.* **1999**, *99*, 3435. (c) Irvine, G. J.; Lesley, M. J. G.; Marder, T. B.; Norman, N. C.; Rice, C. R.; Robins, E. G.; Roper, W. R.; Whittell, G. R.; Wright, L. J. *Chem. Rev.* **1998**, *98*, 2685. (d) Beletskaya, I. P., Pelter, A. *Tetrahedron* **1997**, *53*, 4957. (e) Burgess, K.; Ohlmeyer, M. J. *Chem. Rev.* **1991**, *91*, 1179. (f) Baker, R. T.; Nguyen, P.; Marder, T. B.; Westcott, S. A. *Angew. Chem., Int. Ed. Engl.* **1995**, *34*, 1336.

(3) Han, L.; Tanaka, M. *Chem. Commun.* **1999***, 395.* (c) Miyaura, N.; Suzuki, A. *Chem. Rev.* **1995**, *95*, 2457. (a) Musaev, D. G.; Mebel, A. M.; Morokuma, K. *J. Am. Chem. Soc.* **1994**, *116*, 10693.

(4) (a) Kondo, T.; Mitsudo, T. *Chem. Rev*. **2000**, *100*, 3205. (b) Beletskaya, I.; Moberg, C. *Chem. Rev.* **1999**, *99*, 3435. (c) Ogawa, A. *J. Organomet. Chem*. **2000**, *611*, 463. (d) Sugoh, K.; Kuniyasu, H.; Sugae, T.; Ohtaka, A.; Takai, Y.; Tanaka, A.; Machino, C.; Kambe, N.; Kurosawa, H. *J. Am. Chem. Soc*. **2001**, *123*, 5108. (e) Kuniyasu, H.; Ohtaka, A.; Nakazono, T.; Kinomoto, M.; Kurosawa, H. *J. Am. Chem. Soc*. **2000**, *122*, 2375. (f) Ogawa, A.; Kawakami, J.; Mihara, M.; Ikeda, T.; Sonoda, N.; Hirao, T. *J. Am. Chem. Soc.* **1997**, *119*, 12380. (g) Xiao, W.; Alper, H. *J. Org. Chem*. **2001**, *66*, 6229. (h) Ishii, A.; Saito, M.; Murata, M.; Nakayama, J. *Eur. J. Org. Chem*. **2002**, 979.

(5) Han, L.; Tanaka, M. *J. Am. Chem. Soc.* **1998**, *120*, 8249.

(6) Ogawa, A.; Kudo, A.; Hirao, T. *Tetrahedron Lett*. **1998**, *39*, 5213.

(7) (a) Ananikov, V. P.; Beletskaya, I.; Aleksandrov, G. G.; Eremenko, I. L. *Organometallics* **2003**, *22*, 1414. (b) Ananikov, V. P.; Kabeshov, M. A.; Beletskaya, I. P.; Aleksandrov, G. G.; Eremenko, I. L. *J. Organomet. Chem*. **2003**, *687*, 451.

(8) Albano, V. G.; Monari, M.; Orabona, I.; Panunzi, A.; Ruffo, F. *J. Am. Chem. Soc.* **2001**, *123*, 4352.

10.1021/om050023s CCC: $30.25
Publication on Web 09/15/2005

Scheme 1. Presentation of the Studied Reactions

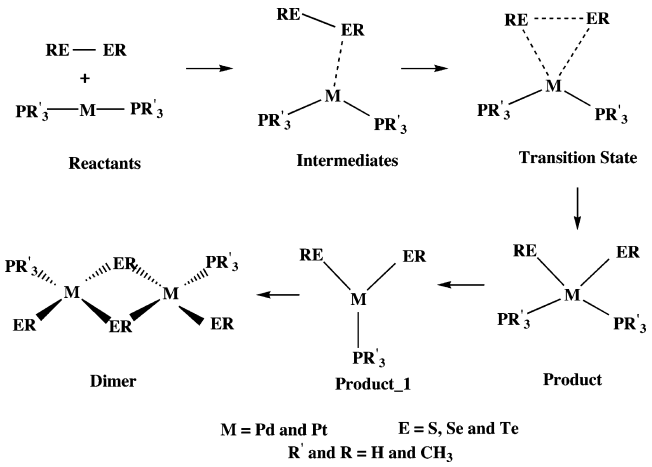

factors controlling these fascinating reactions. The solution to these problems requires comprehensive investigations. In the present paper, we study the mechanisms and factors controlling the oxidative addition of S−S, Se−Se, and Te−Te to the Pd(0) and Pt(0) complexes $M(PR'_3)_2$, using the density functional approach. We believe that these calculations will allow us to elucidate the roles of the chalcogen atoms (E), transition metal centers (Pd and Pt), and auxiliary ligands PR'_3 (see Scheme 1) in the oxidative addition of S−S, Se−Se, and Te−Te bonds to transition metal centers. Here, we report the cases with R, R′ = H, CH_3 (or Me).

II. Computational Methods

The geometries of the reactants, intermediates, transition states, and products of the proposed reactions have been obtained at the B3LYP density functional level,[9] using the slightly modified standard LANL2DZ basis set of Hay and Wadt[10] by augmenting it with an additional set of d functions on the phosphorus, sulfur, selenium, and tellurium atoms, with exponents of $\alpha_d(P) = 0.55$, $\alpha_d(S) = 0.65$, $\alpha_d(Se) = 0.363$, and $\alpha_d(Te) = 0.25$. This basis set will be referred to as LANL2DZ+d. Previously, it was found that the used LANL2DZ+d basis set provides a reasonable agreement with the available experimental data.[11] The nature of all stationary points was confirmed by performing a normal-mode analysis at the 298.15 K, 1 atm, and rigid rotor harmonic oscillator approximation. In addition, the nature of the calculated transition states was clarified using the intrinsic reaction coordinates (IRC) approach. All calculations were performed without any symmetry constraints using the GAUSSIAN 03 quantum chemical package.[12] Throughout the paper the calculated energetics and geometries of the Pd and Pt complexes will be presented without and within brackets, respectively: i.e., in the manner Pd [Pt]. Below, we will use the chemically more interesting ΔG values in the discussion and corresponding ΔH values will be given in parentheses.

(9) (a) Becke, A. D. *Phys. Rev. A* **1988**, *38*, 3098. (b) Lee, C.; Yang, W.; Parr, R. G. *Phys. Rev. B* **1988**, *37*, 785. (c) Becke, A. D. *J. Chem. Phys*. **1993**, *98*, 5648.

(10) (a) Hay, P. J.; Wadt, W. R. *J. Chem. Phys.* **1985**, *82*, 270. (b) Hay, P. J.; Wadt, W. R. *J. Chem. Phys.* **1985**, *82*, 284. (c) Hay, P. J.; Wadt, W. R. *J. Chem. Phys.* **1985**, *82*, 299.

(11) See: *Computational Modeling of Homogeneous Catalysis*; Maseras, F., Lledos, A., Eds.; Kluwer Academic: Dordrecht, The Netherlands, 2002.

(12) Frisch, M. J. et al. *Gaussian 03*, Rev. C1; Gaussian, Inc., Pittsburgh, PA, 2003.

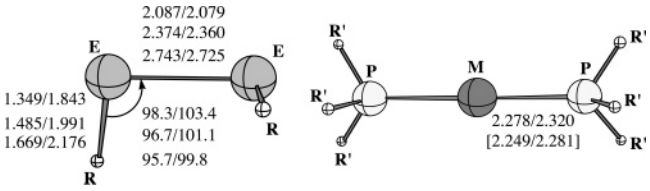

Figure 1. Calculated important geometry parameters of the reactants. Numbers are given before and after the slash belong to R or R′ = H, Me, respectively. The numbers given in the first, second, and third lines correspond to E = S, Se, Te, respectively. The numbers without brackets correspond to M = Pd, while those in brackets correspond to M = Pt. All distances are given in Å and angles in deg.

This paper is organized as follows. At first, in section IIIA, we discuss the oxidative addition reactions

$$RE{-}ER + 2M(PR'_3)_2 \rightarrow \textit{cis}\text{-}(PR'_3)_2M(ER)_2 \qquad (1)$$

Then, in section IIIB, we briefly discuss the second part of the studied reaction, namely, the thermodynamics of the dimerization process

$$2\textit{cis}\text{-}(PR'_3)_2M(ER)_2 \rightarrow (PR'_3)(ER)M(\mu\text{-}ER)_2M(PR'_3)(ER) + 2PR'_3 \qquad (2)$$

Finally, in section IV we draw several conclusions from these studies.

In Figures 1−6 we present reactants, intermediates, and transition states of all the studied reactions along with their important geometry parameters. Full geometry parameters of these structures are given in the Table 1S of the Supporting Information. The relative energies (enthalpy ΔH and Gibbs free energy ΔG at the temperature 298.15 K and pressure 1 atm, calculated relative to the reactants REER + $M(PR'_3)_2$) of the presented structures for reaction 1 are listed in Tables 1 (M = Pd) and 2 (M = Pt). In Table 3, we present the calculated energetics of reaction 2.

III. Results and Discussion

A. Potential Energy Surface of the Oxidative Addition Reaction (1). In general, we have found similar intermediates, transition states, and immediate products for all the calculated reactions (1) regardless of the nature of the chalcogen atoms E (S, Se, and Te), transition-metal centers (Pd and Pt), auxiliary ligands PR'_3 (PH_3 and PMe_3), and ligand substituents R (H and Me). Therefore, below we briefly discuss only the most interesting geometrical features of each of these structures.

i. Geometrical Features of the Reactants, Intermediates, Transition States, and Products of the Reaction RE-ER + $M(PR'_3)_2$ → *cis*-$(PR'_3)_2M(ER)_2$. Reactants. Geometries of reactants of the reaction (1), RE−ER and $M(PR'_3)_2$, are presented in Figure 1. The complex $M(PR'_3)_2$ was the subject of numerous previous studies[13] and will not be discussed in the present paper. For the other reactant, RE−ER, we have found that E−E bond distances are 2.087 and 2.079 Å for E = S, 2.374 and 2.360 Å for E = Se, and 2.743 and 2.725 Å for E = Te, for R = H and Me, respectively. These

(13) (a) Kitaura, K.; Obara, S.; Morokuma, K. *J. Am. Chem. Soc*. **1981**, *103*, 2891. (b) Low, J. J.; Goddard, W. A., III. *J. Am. Chem. Soc*. **1986**, *108*, 6115. (c) Sumimoto, M.; Iwane, N.; Takahama, T.; Sakaki, S. *J. Am. Chem. Soc*. **2004**, *126*, 10457. (d) Sakaki, S.; Kai, S.; Sugimoto, M. *Organometallics* **1999**, *18*, 4825.

calculated values are in good agreement with the available experimental results for sulfur, namely 2.055 Å[14] for HSSH and 2.038 Å[15] for CH_3SSCH_3.

Intermediates. As can be expected, the intermediates of the reaction RE−ER + $M(PR'_3)_2$ are the weakly bound molecular complexes $(PR'_3)_2M$−(REER), which could have numerous isomers. In this paper, we located two isomers of these complexes for R = R′ = H and Me, called **C_1** and **C_2**, where the REER fragment is bound to the metal center with its E and H atoms, respectively (see Figure 2). Although the **C_2** isomer is calculated to be a few kcal mol^{-1} more stable than **C_1** (see Tables 1 and 2), relative to the dissociation limit of RE−ER + $M(PR'_3)_2$, below we discuss only the isomer **C_1,** because it is on the oxidative addition pathway and expected to be separated from **C_2** by a small energy barrier. We do not expect the existence of **C_2** (as well as **C_1**) will significantly contribute to the mechanism of the overall oxidative addition reaction (1) because they are very weakly bound complexes, and most likely reactions start directly from the corresponding reactants. Close examination of the geometrical parameters of **C_1** shows that the interaction of the RE−ER and $M(PR'_3)_2$ fragments slightly (by 0.05−0.10Å) elongates the E−E bond distance and bends the P−M−P angle from 180° to about 120°. The E−E bond elongation (relative to the reactant) is slightly larger for PR'_3 = PMe_3 than for PR'_3 = PH_3.

Oxidative Addition Transition State. Oxidative addition of the RE−ER bond to the transition-metal center (Pd and Pt) occurs via the transition state **TS**, given in Figure 3. As seen from this figure, at the **TS** the to-be-broken E−E bond is already significantly elongated by 0.07−0.32 Å. In general, these changes are slightly larger for R, R′ = H than for R, R′ = Me and for M = Pt than for M = Pd. Interestingly, the nascent M−E bonds are slightly longer in **TS** than in **C_1**. The normal-mode analyses show that all **TS**'s are real transition states with one imaginary frequency and connect **C_1** with the product *cis*-$(PR'_3)_2M(ER)_2$. Furthermore, it is apparent that at **TS** the E−E vector is roughly perpendicular to the P−M−P plane, which is consistent with previous findings.[16]

Product Species *cis*-$(PR'_3)_2M(ER)_2$. Overcoming the transition state, **TS,** leads to the formation of the product complex *cis*-$(PR'_3)_2M(ER)_2$. However, as shown experimentally,[7] the formed *cis*-$(PR'_3)_2M(ER)_2$ complex is not the final product of the reaction RE−ER + $M(PR'_3)_2$. For M = Pt it isomerizes to *trans*-$(PR'_3)_2M(ER)_2$, while for M = Pd it forms the dimer $(ER)(PR'_3)Pd(\mu\text{-}ER)_2Pd(ER)(PR'_3)$. In this paper we will briefly discuss only the dimerization process (see section IIIB).

As seen in Figure 4, the calculated $(PH_3)_2Pt$−SeH and $(PH_3)_2Pt$−SeMe bond distances are 2.545 and 2.537 Å, which are slightly longer than those, 2.355 and 2.353 Å, for $(PMe_3)_2Pt$−SeH and $(PMe_3)_2Pt$−SeMe, respectively. These calculated numbers are in reasonable agreement with the experimentally reported Pt−Se bond distances of 2.46−2.49[7a] and 2.5142(5) Å. [8]

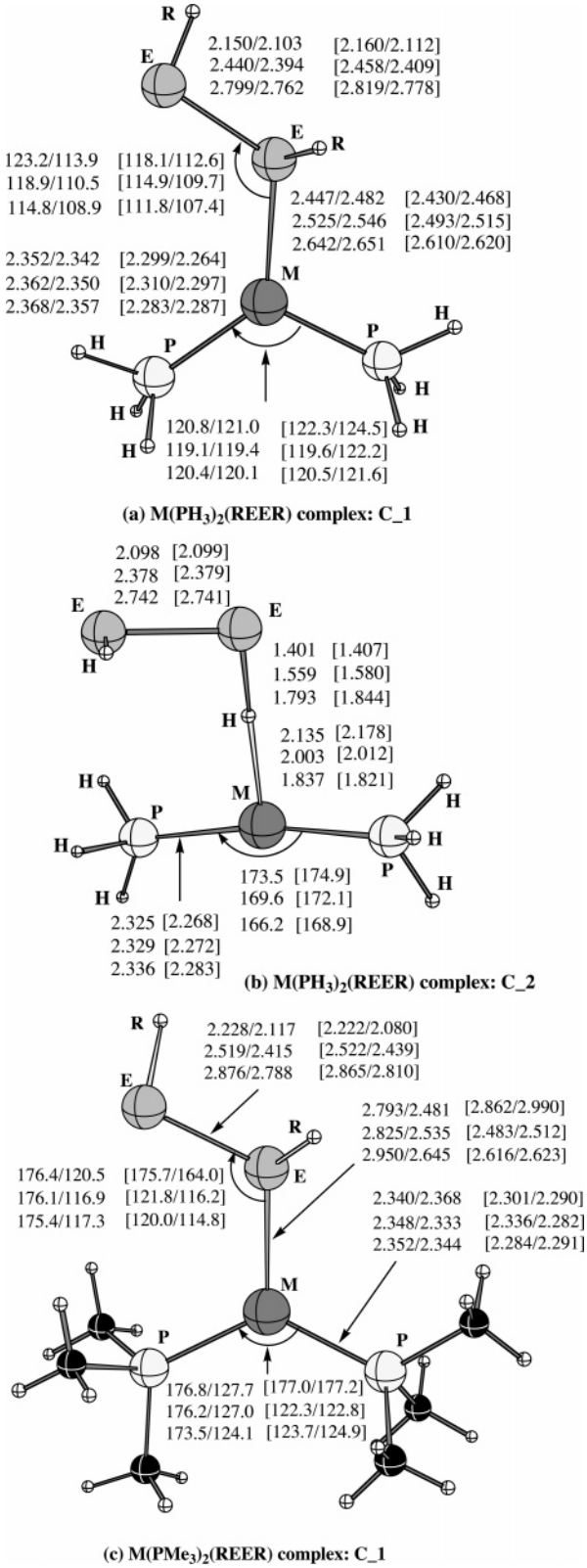

Figure 2. Calculated important geometry parameters of the complex $(PR'_3)_2M(REER)$. See Figure 1 for details.

ii. Potential Energy Surface of the Reaction (1). The calculated relative energies of the aforementioned intermediates, transition states, and products of the reaction RE−ER + $M(PR'_3)_2 \rightarrow$ *cis*-$(PR'_3)_2M(ER)_2$ are given in Tables 1 and 2 for M = Pd, Pt, respectively.

(14) Winnewisser, G.; Winnewisser, M.; Gordy, W. *J. Chem. Phys.* **1968**, *49*, 3465.
(15) Sutter, D.; Dreizler, H.; Rudolph, F. *Z. Naturforsch.* **1964**, *19*, 512.
(16) (a) Cui, Q.; Musaev, D. G.; Morokuma, K. *Organometallics* **1997**, *16*, 1355, (b) Sakaki, S.; Ogawa, M.; Musashi, Y.; Arai, T. *Inorg. Chem.* **1994**, *33,* 1660.

Table 1. Calculated Energetics (Relative to Reactants, in kcal mol^{-1}) of the Intermediates, Transition States, and Products of the Reaction (1) for M = Pd and Different E, R, and R′

	E = S		E = Se		E = Te	
structure	Δ*H*	Δ*G*	Δ*H*	Δ*G*	Δ*H*	Δ*G*
			R = R′ = H			
C_1 (M−E)	−2.45	6.51	−4.58	4.23	−6.77	1.75
C_2 (M−H)	−4.18	4.17	−4.72	3.99	−5.73	2.82
TS	11.94	22.30	3.90	14.78	−3.26	8.05
Prod	−19.99	−7.91	−16.92	−4.83	−13.10	−1.18
			R = R′ = Me			
C_1 (M−E)	1.81	9.60	−0.95	6.27	−3.47	5.14
TS	19.45	29.99	9.74	20.61	1.27	12.26
Prod	−13.58	−1.76	−11.80	0.18	−8.48	3.31
			R = Me and R′ = H			
C_1 (M−E)	−2.23	6.51	−4.60	4.04	−7.64	2.69
TS	15.90	27.73	6.00	17.71	−2.70	8.71
Prod	−8.61	4.40	−8.83	4.03	−8.00	4.92
			R = H and R′ = Me			
C_1 (M−E)	−4.59	3.21	−7.60	0.40	−9.40	−1.01
TS	14.79	24.01	7.18	16.99	−0.16	9.82
Prod	−27.38	−15.51	−21.97	−10.12	−15.46	−3.47

Table 2. Calculated Energetics (Relative to Reactants, in kcal mol^{-1}) of the Intermediates, Transition States, and Products of the Reaction (1) for M = Pt and Different E, R, and R′

	E = S		E = Se		E = Te	
structure	Δ*H*	ΔG	Δ*H*	Δ*G*	Δ*H*	Δ*G*
			R = R′ = H			
C_1 (M−E)	1.77	10.92	-1.62	8.76	-4.08	4.91
C_2 (M−H)	-4.49	4.04	-5.05	3.73	-6.41	1.45
TS	19.62	29.93	10.68	21.55	1.79	13.27
Prod	-27.99	-15.91	-24.07	-12.04	-22.06	-10.55
			R = R′ = Me			
C_1 (M−E)	1.91	11.01	2.46	12.53	-0.29	9.87
TS	27.33	37.73	17.28	28.84	8.00	19.76
Prod	-19.45	-7.27	-16.77	-4.77	-11.70	0.85
			R = Me and R′ = H			
C_1 (M−E)	1.94	11.02	-1.81	8.78	-4.61	3.97
TS	22.56	34.22	11.80	23.41	1.88	14.23
Prod	-16.70	-3.98	-16.17	-3.62	-13.81	-1.09
			R = H and R′ = Me			
C_1 (M−E)	3.22	12.43	2.28	10.91	-0.65	7.31
TS	23.06	32.13	14.63	24.90	5.53	16.14
Prod	-32.28	-20.53	-26.31	-14.55	-24.70	-12.60

Chalcogen Effect. Analyses of the data given in Tables 1 and 2 clearly show that as the energy of the **C_1** complex decrease, the energy of the **TS** decreases as well, but the exothermicity of the reaction 1 also decreases via the trend E = S > Se > Te, for all R, R′, and transition-metal atoms. The obtained trend in the energy of the TS could be partially explained in term of the calculated E−E bonding energy (kcal mol^{-1}) in the RE−ER reactant, which decreases via E = S {43.8 for Δ*G* (52.8 for Δ*H*)} > Se {39.6 (48.5)} > Te {34.1 (42.8)} for R = H and E = S {38.6 (48.9)} > Se {35.4 (47.2)} > Te {31.0 (40.7)} kcal mol^{-1} for R = Me. In other words, *the weaker the E−E bond strength, the smaller the oxidative addition barrier.*

The obtained trend in the overall exothermicity of the reaction, namely that it decreases via the pattern E = S > Se > Te, indicates that the M−ER bond strength decreases via the trend E = S > Se > Te, which is consistent with the trend of the calculated M−ER bond energies (kcal mol^{-1}) in the *cis*-$(PR'_3)_2M(ER)_2$ complex; for M = Pd, R = R′ = H we have found that E = S {33.1 (45.8)} > Se {28.2 (41.2)} > Te {21.5 (35.4)} and for R = R′ = CH_3, E = S {27.5 (42.0)} > Se {23.1 (38.7)} > Te {19.1 (32.5)}. When M = Pt, R = R′ = H the bond energies (kcal mol^{-1}) are E = S {40.8 (54.1)} > Se {35.1 (48.6)} > Te {32.6 (44.6)}, and for R = R′ = CH_3, E = S {37.0 (50.2)} > Se {30.4 (45.7)} > {21.8 (38.1)}. It is noteworthy that the calculated Pt−SeR bond enthalpy (kcal mol^{-1}), (48.6) (for R = R′ = H)) and (45.7) (for R = R′ = Me)), is in reasonable agreement with the value 33 kcal mol^{-1} reported by Albano and co-workers[8] for $Pt(SeMe)_2$(dmphen)(olefin).

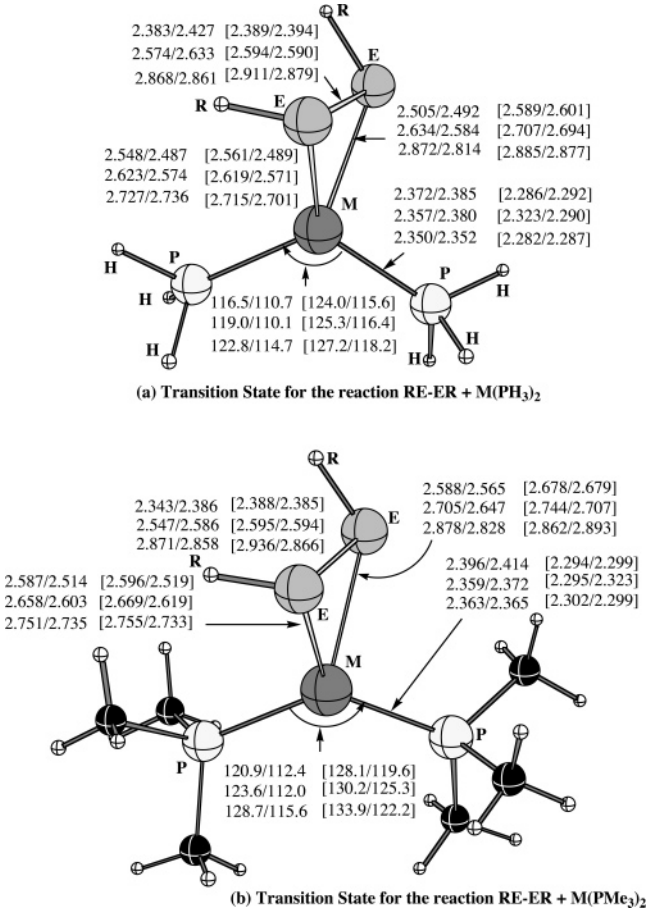

Figure 3. Calculated important geometry parameters of the RE−ER activation transition states. See Figure 1 for details.

Metal Effect. Comparison of the results in Table 1 with those in Table 2 shows that upon going from M = Pd to M = Pt, the complex **C_1** becomes less stable, the E−E activation barrier becomes higher, and the overall reaction becomes more exothermic for all studied R, R′, and E. The trend in the calculated exothermicity of the reaction is a result of the difference in the M−ER bonding energies in the product *cis*-$(PR'_3)_2M(ER)_2$; the Pt−ER bond is stronger than the Pd−ER bond. The different Pd−ligand and Pt−ligand bond energies were previously rationalized and will not be repeated here.[17]

The larger activation barrier for Pt, compared to that for Pd, can be explained in terms of the energy required for deformation of the P−M−P angle from 180 to 120°. The P−Pt−P angle is much more rigid than the P−Pd−P angle. Our calculations show that the energies (kcal

(17) Cui, Q.; Musaev, D. G.; Morokuma, K. *Organometallics* **1998**, *17*, 1383.

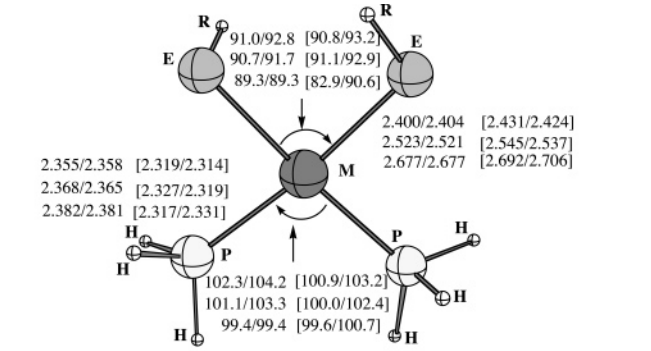

(a) Product of the of the RE-ER oxidative addition to $M(PH_3)_2$

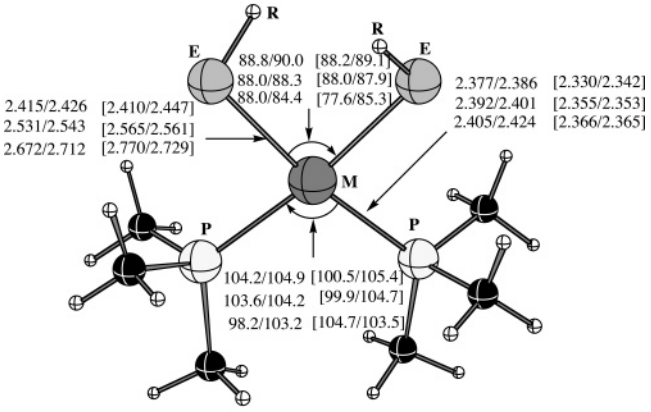

(b) Product of the of the RE-ER oxidative addition to $M(PMe_3)_2$

Figure 4. Calculated important geometry parameters of the product complex $(PR'_3)_2M(RE)_2$. See Figure 1 for details.

mol^{-1}) required to bend this angle from 180 to 120° in $(PH_3)_2Pd$, $(PMe_3)_2Pd$, $(PH_3)_2Pt$, and $(PMe_3)_2Pt$ are 6.6, 9.8, [12.7], and [16.6], respectively, which is consistent with the calculated trend in the E−E activation barriers for M = Pt, Pd. The rigidity of the P−Pt−P angle compared to the P−Pd−P angle is also the reason for the destabilization of the complex **C_1** upon going from the Pt complex to Pd. Thus, the present calculations show that the Pd(0) complex activates the RE−ER bond much more easily than its Pt(0) analogue, which is consistent with the available experimental data.[7]

iii. Roles of R and R′ Substituents in REER and PR′$_3$. At first let us discuss the symmetric cases with R = R′ = H, Me. The presented data show that upon going from R = R′ = H to R = R′ = Me, the **C_1** complex is destabilized, the energy barrier at the **TS** is increased, and the overall energy of the reaction is decreased. As expected, the calculated activation barriers for the asymmetric cases with R ≠ R′ = H, Me are larger than those for the R = R′ = H symmetric systems but are smaller than those for R = R′ = Me systems. *In other words, the more methyl substitution, the larger the activation barrier*. However, the calculated stability of the **C_1** complex and the overall energy of the reaction (1) do not obey this simple rule. Indeed, for R′ = H, the substitution of the H ligands in HEEH by methyl groups does not significantly affect the energetics of **C_1**, while it significantly reduces the exothermicity of the reaction (1) for all studied chalcogen (E) and transition-metal (M) atoms. Meanwhile, for R = H, the substitution of the H ligands in $Pd(PH_3)_2$ by the methyl groups stabilizes both the **C_1** complex and the product of the reaction, *cis*-$(PR'_3)_2Pd(ER)_2$, relative to the reactants for all studied E's. However, these trends in the stability of the **C_1** complex and energy of the reaction (1) for R = H, R′ = H, Me, and M = Pd are different for the M = Pt case: the substitution of the H ligands in $Pt(PH_3)_2$ by the methyl groups while keeping R = H destabilizes the **C_1** complex but stabilizes the product of the reaction, *cis*-$(PR'_3)_2Pt(ER)_2$, relative to the reactants for all studied E's.

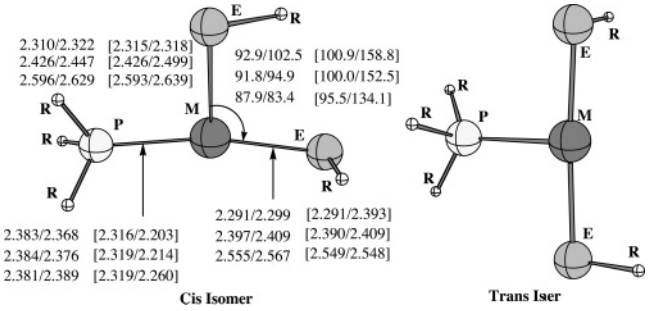

Figure 5. Calculated important geometry parameters of the complex $(PR'_3)M(REER)$ and schematic representations of its cis and trans isomers. See Figure 1 for details.

The calculated trends in the stability of the **C_1** complex and activation barrier could be partially explained by the steric repulsion between the R and R′ groups, which is stronger for the methyl-substituted systems than for the unsubstituted ones. However, the stability of the products relative to the reactants might be strongly influenced by electronic factors: replacing H ligands by Me in HEEH and $M(PH_3)_2$ systems can affect the RE−ER and M−PR′$_3$ bond strengths.

B. Thermodynamics of the Dimerization Reaction (2). As mentioned previously, the experimental studies[7] show that the final product of the reaction of RE−ER with $M(PR'_3)_2$ is not *cis*-$(PR'_3)M(ER)_2$; for M = Pt it is the *trans*-$(PR'_3)_2M(ER)_2$ complex, while for M = Pd it is the dimer $(ER)(PR'_3)Pd(\mu\text{-}ER)_2Pd(ER)(PR'_3)$. Here we discuss only the dimerization process, which can proceed via two different pathways, dissociative and assiociative: the dissociative pathway starts with the dissociation of one of the PR′$_3$ ligands from *cis*-$(PR'_3)_2M(ER)_2$ to give the coordinatively unsaturated complex $(PR'_3)M(ER)_2$, which later dimerizes to give the final product $(ER)(PR'_3)Pd(\mu\text{-}ER)_2Pd(ER)(PR'_3)$. Meanwhile, the associative pathway starts with cis−trans isomerization of the directly formed *cis*-$(PR'_3)M(ER)_2$ structure followed by dimerization of the trans product to form $(ER)(PR'_3)Pd(\mu\text{-}ER)_2Pd(ER)(PR'_3)$. Here we only report the thermodynamics for dissociative pathway of symmetric systems with R = R′ = H, Me. More detailed studies of the dimerization of *cis*-$(PR'_3)M(ER)_2$ are in progress.

i. The Reaction *cis*-$(PR'_3)_2M(ER)_2 \rightarrow$ *cis*-$(PR'_3)M(ER)_2$ + PR′$_3$. Let us start our discussion with the phosphine dissociation reaction: *cis*-$(PR'_3)_2M(ER)_2 \rightarrow (PR'_3)M(ER)_2 + PR'_3$. The product of this reaction, $(PR'_3)M(ER)_2$, in general, may have two different isomers, trans and cis. *cis*-$(PR'_3)M(ER)_2$ is found to be the isomer lowest in energy (by 2−4 kcal mol^{-1}) in all studied cases except for M = Pt and R = R′ = Me, for which the trans isomer is energetically lowest, and the cis isomer is not a minimum on the potential energy surface (see Figure 5). As seen in Figure 5, upon going

Table 3. Calculated Energetics of the Reactions (kcal mol^{-1}) 2*cis*-(PR′$_3$)M(ER)$_2$ → (ER)(PR′$_3$)Pd(μ-ER)$_2$Pd(ER)(PR′$_3$) and *cis*-(PR′$_3$)$_2$M(ER)$_2$ → *cis*-(PR′$_3$)M(ER)$_2$ + PR′$_3$

	R = H		R = Me	
E	ΔH	ΔG	ΔH	ΔG
2 *cis*-(PR′$_3$)M(ER)$_2$ → (ER)(PR′$_3$)Pd(μ-ER)$_2$Pd(ER)(PR′$_3$)				
		M = Pd		
S	−46.2	−32.3	−48.2	−30.5
Se	−45.2	−30.6	−43.8	−26.6
Te	−38.8	−25.3	−35.5	−18.5
		M = Pt		
S	−56.1	−41.4	−43.3	−24.4
Se	−51.7	−36.8	−41.4	−24.2
Te	−45.7	−36.5	−40.0	−23.8
cis-(PR′$_3$)$_2$M(ER)$_2$ → *cis*-(PR′$_3$)M(ER)$_2$ + PR′$_3$				
		M = Pd		
S	18.6	7.4	23.7	9.9
Se	16.0	4.7	20.4	6.3
Te	12.0	0.8	15.1	1.2
		M = Pt		
S	25.6	13.6	25.3	10.2
Se	22.3	11.0	22.4	8.2
Te	20.8	10.3	19.0	5.1

from R = R′ = H to R = R′ = Me, the E−M−E angle increases because of steric repulsion between the Me groups. In general this angle is larger for M = Pt than for M = Pd.

As seen in Table 3, the calculated endothermicity (kcal mol^{-1}) of the reaction *cis*-(PR′$_3$)$_2$Pd(ER)$_2$ → *cis*-(PR′$_3$)Pd(ER)$_2$ + PR′$_3$ for E = S, Se, Te, respectively, is S {18.6 (7.4)} > Se {16.0 (4.7)} > Te {12.0 (0.8)} for R = R′ = H and S {23.7 (9.9)} > Se {20.4 (6.3)} > Te {15.1 (1.2)} kcal mol^{-1} for R = R′ = Me. For the M = Pt, these values are {25.6 (13.6)} > {22.3 (11.0)} > {20.8 (10.3)} for R = R′ = H and {25.3 (10.2)} > {22.4 (8.2)} > {19.0 (5.1)} for R = R′ = Me. In other words, the endothermicity of the reaction decreases (a) via E = S > Se > Te for given M and R = R′ and (b) via M = Pt > Pd for given E and R = R′. Interestingly, PR′$_3$ dissociation from *cis*-(PR′$_3$)$_2$M(ER)$_2$ is more significantly affected by the R to R′ substitution for M = Pd than for M = Pt.

ii. The Dimerization Reaction 2(PR′$_3$)M(ER)$_2$ → (ER)(PR′$_3$)Pd(μ-ER)$_2$Pd(ER)(PR′$_3$). Dimerization of the resultant (PR′$_3$)M(ER)$_2$ intermediate may proceed via the transition state required for the reorganization of the monomer (PR′$_3$)M(ER)$_2$. However, in this paper we have not calculated this transition state, primarily because the energy of the reaction *cis*-(PR′$_3$)$_2$Pd(ER)$_2$ → *cis*-(PR′$_3$)Pd(ER)$_2$ + PR′$_3$, leading to the precursor complex (PR′$_3$)M(ER)$_2$, clearly is higher (ca. 7 kcal mol^{-1}; see Table 3) for Pt systems than for Pd. This indicates that the dimerization process is going to be less feasible for Pt systems that Pd ones, which is in agreement with the experimental observations.[7]

The precursor (PR′$_3$)M(ER)$_2$ may have two isomers, cis and trans, and the reported dimerization energy was calculated relative to the cis isomer.

As shown in Chart 1, the dimer (ER)(PR′$_3$)Pd(μ-ER)$_2$-Pd(ER)(PR′$_3$) may have several isomers that differ in the positions of the RE and PR′$_3$ ligands (given by the first label below), as well as by the positioning of the R substituents in the two RE ligands (the second label), namely, ***cis*−*cis***, ***cis*−*trans***, ***trans*−*cis***, and ***trans*−*trans***. Detailed analysis of these structures for M = Pd

Chart 1. Presentation of the Calculated Structures of the Dimer (PR′$_3$)(ER)M(μ-ER)$_2$M(ER)(PR′$_3$)

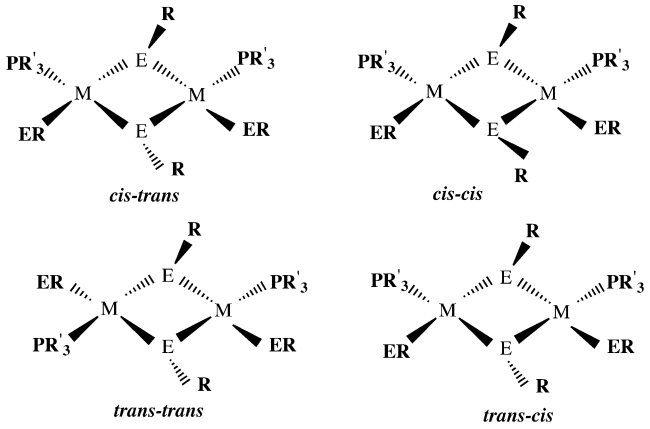

shows that the ***trans*−*cis*** and ***cis*−*cis*** structures are higher in energy than the ***cis*−*trans*** and ***trans*−*trans*** isomers by 8−9 kcal mol^{-1}. Since the low-energy structures, ***cis*−*trans*** and ***trans*−*trans***, are very close in energy, within 1−2 kcal mol^{-1}, in our discussion below we will use only the ***cis*−*trans*** isomer for both M = Pd and M = Pt.

The geometry of the ***cis*−*trans*** isomer is given in Figure 6. The corresponding dimerization energies, i.e., the energies of the reaction *cis*-(PR′$_3$)M(ER)$_2$ → (ER)-(PR′$_3$)Pd(μ-ER)$_2$Pd(ER)(PR′$_3$), are summarized in Table 3. As seen in Table 3, for M = Pd, the calculated energy (kcal mol^{-1}) of dimerization decreases in the order E = S {32.3 (46.2)} > Se {30.6 (45.2)} > Te {25.3 (38.8)} for R = R′ = H and {30.5 (48.2)} > {26.6 (43.8)} > {18.5 (35.5) for R = R′ = Me. For M = Pt, these energies (kcal mol^{-1}) are {41.4 (56.1)} > {36.8 (51.7)} > {36.5 (45.7)} for R = R′ = H and {24.4 (43.3)} > {24.2 (41.4)} > {23.8 (40.0)} kcal mol^{-1} for R = R′ = Me. Thus, the energy for the dimerization of *cis*-(PR′$_3$)M(ER)$_2$ decreases via the trend E = S > Se > Te and increases via M = Pd < Pt for R = R′ = H. For the R = R′ = Me case, the first trend (for E) remains the valid, and the second trend (for M) is less profound.

The exothermicity (kcal mol^{-1}) of the entire process 2(PR′$_3$)$_2$M + REER → (ER)(PR′$_3$)Pd(μ-ER)$_2$Pd(ER)(PR′$_3$) is calculated to be S {33.3 (48.9)} > Se {30.8 (47.0)} >

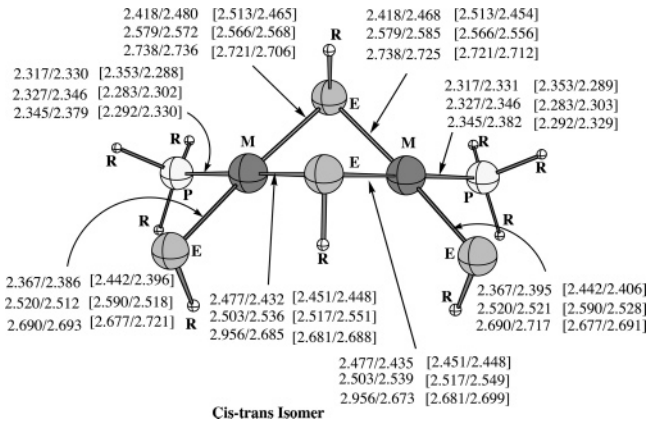

Figure 6. Calculated important geometry parameters of the energetically lowest ***cis*−*trans*** isomer of the (ER)-(PR′$_3$)Pd(μ-ER)$_2$Pd(ER)(PR′$_3$) dimer. See Figure 1 for details.

Te {26.2 (41.0)} for R = R′ = H and {10.9 (29.3)} > {9.9 (27.8)} > {5.8 (23.6)} kcal mol^{-1} for R = R′ = Me. For Pt these energetics are S {46.0 (61.0)} > Se {40.3 (55.3)} > Te {35.7 (48.3)] for R = R′ = H and {18.6 (31.7)} > {17.5 (30.1)} > {12.1 (25.4)} for R = R′ = Me. Thus, the exothermicity of this reaction is larger for the M = Pt than for the M = Pd complex, for both R = R′ = H and R = R′ = Me.

The energetics presented above clearly show that the lack of the dimer structures for M = Pt during the reaction of S−S and Se−Se with the Pt(0) complex, observed by experimentalists,[7] is not dictated by the energy of dimerization. Rather, we believe the controlling step to be PR'_3 dissociation from the *cis*-$(PR'_3)M(ER)_2$ intermediate. We presume that the cost of formation of this intermediate is a strong thermodynamic retarding force, resulting in a very high barrier to formation for the platinum dimer, while for palladium the effect is less limiting.

IV. Conclusions

From the results presented above, one may draw the following conclusions.

1. The E−E activation barrier by $M(PR'_3)_2$ correlates with the E−E bond energy and decreases via the sequence E = S > Se > Te, for all R, R′, and transition metals studied here; the weaker the E−E bond strength, the smaller the oxidative addition barrier. The overall exothermicity of the reaction (1) also decreases via the same trend, E = S > Se > Te, which correlates with the decrease in the M−ER bond strength. Meanwhile, the E−E activation barrier is found to be higher for M = Pt than for M = Pd, while for all studied R, R′, and E the overall reaction (1) is more exothermic for M = Pt than M = Pd.

2. Upon going from R = R′ = H to R = R′ = Me, the E−E activation barrier increases and the overall exothermicity of the reaction (1) decreases. For the asymmetric cases with one methyl substituent, the activation barriers are between that with no methyl and that with two methyls. It is concluded that the greater the methyl substitution, the larger the activation barrier.

3. The calculated endothermicity of the reaction *cis*-$(PR'_3)_2Pd(ER)_2 \rightarrow$ *cis*-$(PR'_3)Pd(ER)_2 + PR'_3$ decreases (a) via E = S > Se > Te for given M and R = R′, and (b) via M = Pt > Pd for given E and R = R′.

4. The dimerization energy of the resultant *cis*-$(PR'_3)M(ER)_2$ intermediate decreases via the sequence E = S > Se > Te and increases via M = Pd < Pt for R = R′ = H. For the R = R′ = Me case, while the first trend (for E) remains valid, the second trend (for M) is less profound. The exothermicity of this reaction is larger for M = Pt than for M = Pd, for both R = R′ = H and R = R′ = Me.

Acknowledgment. We acknowledge the use of computational facilities at the Emerson Center for Scientific Computing. The present research has in part sbeen upported by a grant (No. CHE-0209660) from the National Science Foundation.

Supporting Information Available: Tables giving the Cartesian coordinates of all of the structures discussed in this paper (Table 1S). This material is available free of charge via the Internet at http://pubs.acs.org.

OM050023S